Available online at www.sciencedirect.com
SCIENCE DIRECT
Journal of Catalysis 238 (2006) 221–231
JOURNAL OF CATALYSIS
www.elsevier.com/locate/jcat

Ti(IV)/trialkanolamine catalytic polymeric membranes: Preparation, characterization, and use in oxygen transfer reactions

Maria Giovanna Buonomenna [a,*], Enrico Drioli [a], Renzo Bertoncello [b], Laura Milanese [b], Leonard J. Prins [b], Paolo Scrimin [a,b], Giulia Licini [b]

[a] *ITM-CNR, via Bucci 17/C, I-87030 Arcavacata Di Rende, CS, Italy*
[b] *Dipartimento Scienze Chimiche, Università di Padova, ITM-CNR, sezione di Padova, via Marzolo 1, I-35131, Padova, Italy*

Received 10 October 2005; revised 29 November 2005; accepted 29 November 2005

Abstract

New heterogeneous oxidation catalysts have been obtained by entrapping Ti(IV)/trialkanolamine complexes within polymeric membranes. The catalytic membranes were prepared by a nonsolvent-induced phase-inversion technique. Three polymers, polyvinylidene fluoride (PVDF), a modified polyetherketone (PEEK-WC), and polyacrylonitrile (PAN), with different functional groups and chemical–physical properties, were used to tune the reactivity of the catalytic polymeric membranes in the stereoselective oxidation to sulfoxide and chemoselective oxidation of secondary amines to nitrones by alkyl hidroperoxides. The chemical–physical analysis of the new catalytic membranes was carried out by SEM, EDX, IR, CAM, and XPS techniques. In particular, the XPS spectra showed a very interesting orientation effect of PVDF membranes on the entrapped Ti(IV)/trialkanolamine complex. PVDF-based catalytic membranes gave the best results, affording products in shorter reaction times, higher yields, and better selectivity compared with the corresponding homogeneous systems. The membranes can be recycled up to five runs with no loss of activity.

Keywords: Catalytic polymeric membranes; Ti(IV)/trialkanolamines complex; Polyvinylidene fluoride

1. Introduction

Most industrial catalysts are high-surface area solids onto which an active component is dispersed in the form of very small particles. To produce selectivities approaching 100%, heterogeneous catalysts will need to share a key characteristic with the homogeneous and biological catalyst: they must present uniform sites and uniform contact patterns as an additional catalyst engineering constraint [1,2].

The capability to produce a well-defined, porous matrix that can serve as catalyst support from a wide variety of inorganic materials is contributing to the production of single-site catalysts in which all of the active sites closely resemble each other [3–7]. From this perspective, homogeneous catalysts entrapped in polymeric membranes represent a situation in which single site heterogeneous catalysts (SSHCs) may be designed.

At low temperature (from room temperature up to about 150 °C), polymeric membranes have some advantages over the most expensive inorganic membranes made from ceramic or metals. Most of the polymers can be easily manufactured in different shapes (e.g., hollow, spiral wound, flat sheet); they are elastic, resist fatigue, have satisfactory diffusion and sorption coefficients, and can be produced with incorporated catalysts as nanosized dispersed metallic clusters [8,9], zeolites and activated carbons [10], or metallic complexes [11–13].

Polydimethylsiloxane (PDMS) is the most widely used polymer system for catalytic polymeric membranes, combining high thermal and mechanical stability with chemical resistance [14]. This dense hydrophobic elastomer has been applied successfully in the immobilization of oxygenation catalysts such as metallo porphyrins [15], epoxidation catalysts such as Mn-salen

* Corresponding author.
E-mail address: mg.buonomenna@itm.cnr.it (M.G. Buonomenna).

0021-9517/$ – see front matter
doi:10.1016/j.jcat.2005.11.044

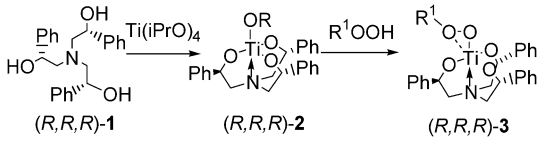

Scheme 1.

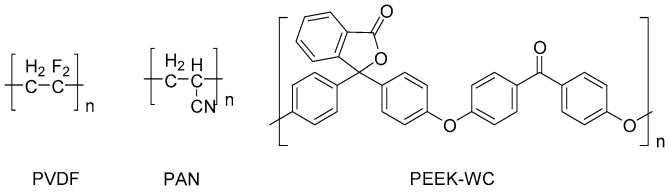

Scheme 2.

[16,17], and Mn-bipyridines in zeolite [18]. The hydrophobicity of the polymer favors the sorption of apolar components, resulting in the suppression of the oxidant decomposition.

This paper describes and discusses the preparation of new catalytic membranes incorporating Ti(IV) complex and their successful use in two model reactions, the sulfoxidation of sulfides to sulfoxides and the secondary amines oxidation to nitrones.

Chiral sulfoxides are an important class of compounds that have increasing applications as chiral auxiliaries in asymmetric synthesis [19] and recently as biological active molecules [20]. The oxidation of amines to nitrones is a very appealing reaction because of the relevance of the metabolic fate of these compounds in vivo and the synthetic interest of the reaction products. Important enzymes are involved in the metabolic oxidation of amines. For example, flavin mono-oxygenase and related compounds, such as 5-ethyl-4a-hydro-peroxyflavin, oxidize secondary amines to nitrones [21]. The simulation of the activity of these enzymes using metal complexes is of great interest, potentially providing mimetic methods for catalytic oxidation of the amines [22].

We have recently reported that tetradentate alkoxide ligands, namely C_3-symmetric trialkanolamines **1** (Scheme 1), provide very stable Ti(IV) homogeneous complexes [23,24]. In the presence of alkyl hydroperoxides, such species are able to catalyze the asymmetric sulfoxidation of alkyl aryl sulfides with ee's up to 84% and with unprecedented catalytic efficiency, reaching turnover numbers (TONs) of 1000 [25] as well as the oxidation of secondary amines to nitrones with high chemoselectivities, quantitative yields, and TONs up to 1400 [26]. Besides the fact that in both cases the oxygen transfer process affords corresponding products with high chemical yields and good selectivities, the Ti(IV) catalyst was shown to be robust under the reaction conditions, which require the presence of large quantities of alkylperoxide [23]. In addition, it affords a stoichiometric amount of water in the case of secondary amine oxidation [24]. Therefore, titanatrane complex **2** seems to be a good candidate for preparing Ti(IV) polymeric catalytic membranes to be used in selective oxygen transfer reactions. They should survive in the conditions required for membrane synthesis because of their intrinsic stability. The membranes are prepared using polymers with different hydrophobicity/hydrophilicity properties: a fluoropolymer, polyvinylidene fluoride (PVDF), modified polyetheretherketone (PEEK-WC) and hydrophilic polyacrylonitrile (PAN) (Scheme 2). All of these polymers are chemically stable in the reaction conditions used.

2. Experimental

2.1. Chemicals

Commercially available reagents and solvents were used as received without further purification for the preparation of polymeric catalytic membranes. PEEKWC was supplied by the Chanchung Institute of Applied Chemistry, Academia Sinica. PVDF 20 10 Solef was supplied by Solvay, Inc. PAN was supplied from SNIA. Ti-**2** was prepared as described previously [23]. Cumene hydroperoxide (Fluka) was stored under molecular sieves at 0 °C. 1,2-dichloroethane was washed three times with 10% H_2SO_4 and with several time until pH reached 7, dried overnight over $CaCl_2$ distilled over P_2O_5, and stored over molecular sieves.

2.2. Preparation of catalytic polymeric membranes

Flat-sheet PVDF-, PAN-, and PEEKWC-based membranes were prepared by phase-inversion process induced by nonsolvent. The membranes were prepared using dimethylacetammide (DMA) as a solvent and distilled water as a nonsolvent. For each polymer, a solution (10.0 wt%) was prepared by dissolving the polymer in DMA (74 wt%) by magnetic stirring at room temperature; then Ti(IV)/trialkanolamine complex (16 wt%) was added, and the resulting solution was stirred for an additional 24 h. The solution was cast on a glass plate by setting the knife gap at 250 μm, and the cast film was immediately immersed for 10 min in a coagulation bath containing distilled water at 15 °C. The membranes were removed from the coagulation bath and stored in distilled water for 24 h to completely remove DMA. Then the membranes were dried in an oven at 60 °C under vacuum for 24 h.

An additional preparation method was used to prepare PVDF-based catalytic membranes using a mixture of two solvents, DMA and acetone; and water as a nonsolvent, following the procedure reported by Pintauro et al. [27]. A solution (10.0 wt%) was prepared by dissolving the polymer in DMA (20 wt%) and Acetone (54 wt%) by magnetic stirring at room temperature; then Ti(IV)/trialkanolamine complex (16 wt%) was added and the resulting solution was left under stirring for additional 24 h at 60 °C. The solution was cast on a glass plate by setting the knife gap at 250 μm, and the cast film was kept at air for 3 h. The membrane was immersed in a coagulation bath containing distilled water at 15 °C. After the membranes were removed from the coagulation bath, the procedure above reported was followed.

2.3. Phase diagrams of the Ti-2/water/DMA/PVDF system

Phase diagrams, at room temperature (ca. 20 °C), were determined by visual observation of the cloud point during slow addition of the nonsolvent to the stirred polymer solution containing Ti-**2**.

2.4. Membrane characterisation

The formed membranes were characterized by the following methods:

(1) The morphology of the membranes was evaluated by means of SEM at 20 kV (Cambridge Instruments Stereoscan 360).
(2) The success of Ti-**2** entrapment and its uniform dispersion in the different polymeric membranes was evaluated by EDX and BSE techniques. EDX microanalyses were performed using a Philips EDAX analysis system.
(3) X-Ray diffractograms were collected by positioning the PVDF films on a sample holder mounted on the Philips PW 1820 powder diffractometer, using Cu-Kα radiation, with the generator working at 40 kV and 40 mA. Intensities were measured in the range $15° < 2\theta < 55°$, typically with step scans of 0.01° (10 s/step). Only the region $15° < 2\theta < 35°$ was analyzed (the outermost region being quite noisy and featureless for all the samples).
(4) FTIR spectra of the prepared films were recorded with a Perkin–Elmer Spectrum One in the range of 4000–400 cm^{-1}.
(5) Information about the chemical state, quantitative surface analyses, and depth profiles were obtained by an XPS spectrometer (Φ 5600 ci; Perkin–Elmer) equipped with Al/Mg anodes working with Al-K_α (1486.6 eV) and Mg-K_α (1253.6 eV) sources at 20 mA and 14 kV. The analyzed areas were 0.8-mm-diameter circles, and the working pressure was about 10^{-7} Pa. The take-off angle was varied between 45° and 15° to obtain different analysis depths (angle-resolved XPS). The quantitative analysis data are reported as atomic percentage of elements.
(6) The acid and base components of the membrane surface tension were obtained by contact angle measurements. Contact angles of various test liquid droplets on the membrane surfaces were measured by the sessile drop method using a CAM 200 contact angle meter (KSV Instruments, Helsinki, Finland). Three reference liquids (distilled water, diiodomethane, and glycerol) were used to determine the apolar γ^{LW}, acid–base γ^{ab}, acid (electron acceptor) γ^+, and base (electron donor) γ^- components of surface free energy by the Good–van Oss–Chaudhury method [28]. The Lifshitz–van der Waals component, γ^{LW}, of the membrane surface tension, reflecting the dipole interactions, was calculated from the measured diiodomethane contact angles under the assumption that diiodomethane is an apolar test liquid,

$$\gamma_s^{LW} = \gamma_l^{LW}(1+\cos\vartheta)^2/4.$$

Table 1
Surface tension parameters for different test liquids according to van Oss, Chaudhury, and Good a 20 °C: γ^{LW} = Lifshitz–van der Waals component, γ^-, γ^+ = electron donor or proton acceptor (basicity or acidity parameters) components of the liquid surface tension γ_S for different test liquids [28,29]

Test liquid	γ (mJ/m^2)	γ^{LW} (mJ/m^2)	γ^{AB} (mJ/m^2)	γ^- (mJ/m^2)	γ^+ (mJ/m^2)
Water	72.8	21.8	51.0	25.5	25.5
Glycerol	64	34	30	3.92	57.4
Diiodomethane	50.8	50.8	0	–	–

Once the γ^{LW} of membrane surface has been measured, it is possible to calculate the other components (γ^{ab}, γ^+, and γ^-) using two polar liquids, as glycerol and water,

$$\gamma_l(1+\cos\vartheta) = 2\left(\left(\gamma_s^{LW}\gamma_l^{LW}\right)^{0.5} + (\gamma_s^+\gamma_l^-)^{0.5} + \left(\gamma_s^-\gamma_l^+\right)^{0.5}\right)$$

and

$$\gamma_s^{ab} = 2(\gamma_s^+\gamma_s^-)^{0.5}.$$

The values of surface tension components of the liquids used in the experiments were taken from the literature [28,29] and are summarized in Table 1.

2.5. Reaction procedures

The performance of the catalytic membranes was investigated under batch conditions using an equal active surface and comparable total catalyst loading. A typical procedure for oxidation of sulfides is as follows. Benzylphenylsulfide (0.1 mmol) is dissolved in dry 1,2-dichloroethane, in a 1.0-mL volumetric flask with an amount of polymer membrane containing 0.01 mmol of Ti-**2**. After cooling at 0 °C, cumylhydroperoxide (CHP) (0.1 mmol) is added under magnetic stirring. The course of the reaction was monitored by gas chromatography (Varian GC equipped with a SE-30 column) and HPLC (*R*,*R*-Dach DNB; *n*-hexene:isopropanol 80:20).

For oxidation of secondary amines, the substrate (0.1 mmol) was dissolved in $CDCl_3$ (or CD_3CN), in a 1.0 ml volumetric flask containing activated molecular sieves (25 mg/mmol) and an amount of polymer membrane containing 0.01 mmol of Ti-**2**. After 30 min, CHP (0.4 mmol) was added. Then the solution was transferred in a screw cap NMR tube and warmed to the reaction temperature, and the course of the reaction was monitored by ^{1}H NMR.

3. Results and discussion

3.1. Phase diagram of Ti-2/water/DMA/PVDF system

The experimental phase diagram of the Ti-**2**/water/DMA/PVDF system is shown in Fig. 1. Line 0% represents the gelation-phase boundary with no catalyst being added. The measured crystallization-induced gelation agrees with data reported by Bottino et al. [30]. On addition of catalyst, the gelation line shifts toward nonsolvent axis and the homogeneous

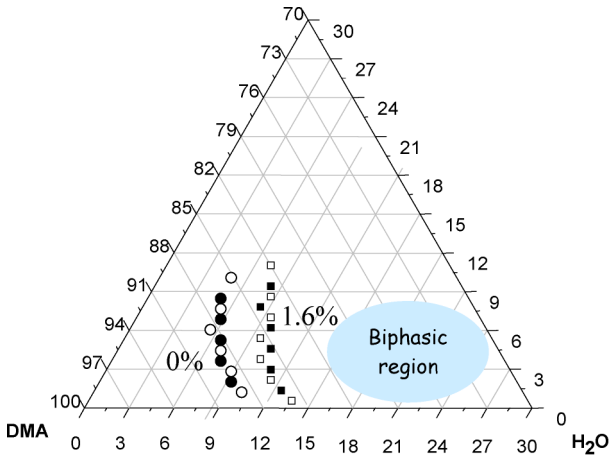

Fig. 1. Phase diagrams of Ti-**2**/DMA/PVDF/water systems at 20 °C. (Ti-**2** content: 0 and 1.6 wt%) determined by visual cloud point observation at room temperature. Closed symbols represent the clear–turbid transition upon nonsolvent addition, open symbols represent the turbid–clear transition upon solvent addition.

solution (one phase) region becomes larger. Such a shift of the binodal demixing curve to higher nonsolvent concentrations is often related to a reduced solvent–nonsolvent interaction and typically leads to delayed demixing [31,32]. In our case, this suggests that in the presence of Ti-**2**, PVDF becomes more soluble in DMA solvent. This is probably due to specific interactions between the catalyst and fluoride groups of the polymer. Some polymer/solvent systems have been reported to exhibit this behavior using salts as additives in a casting solution [33].

3.2. Membrane morphology and catalyst distribution

The Ti-**2** complex has been entrapped in different polymeric membranes using the phase-inversion technique induced by nonsolvent. Some examples of asymmetric membranes prepared by PVDF, PEEKWC and PAN using nonsolvent induced phase-inversion technique have been reported previously [30–33,36–47].

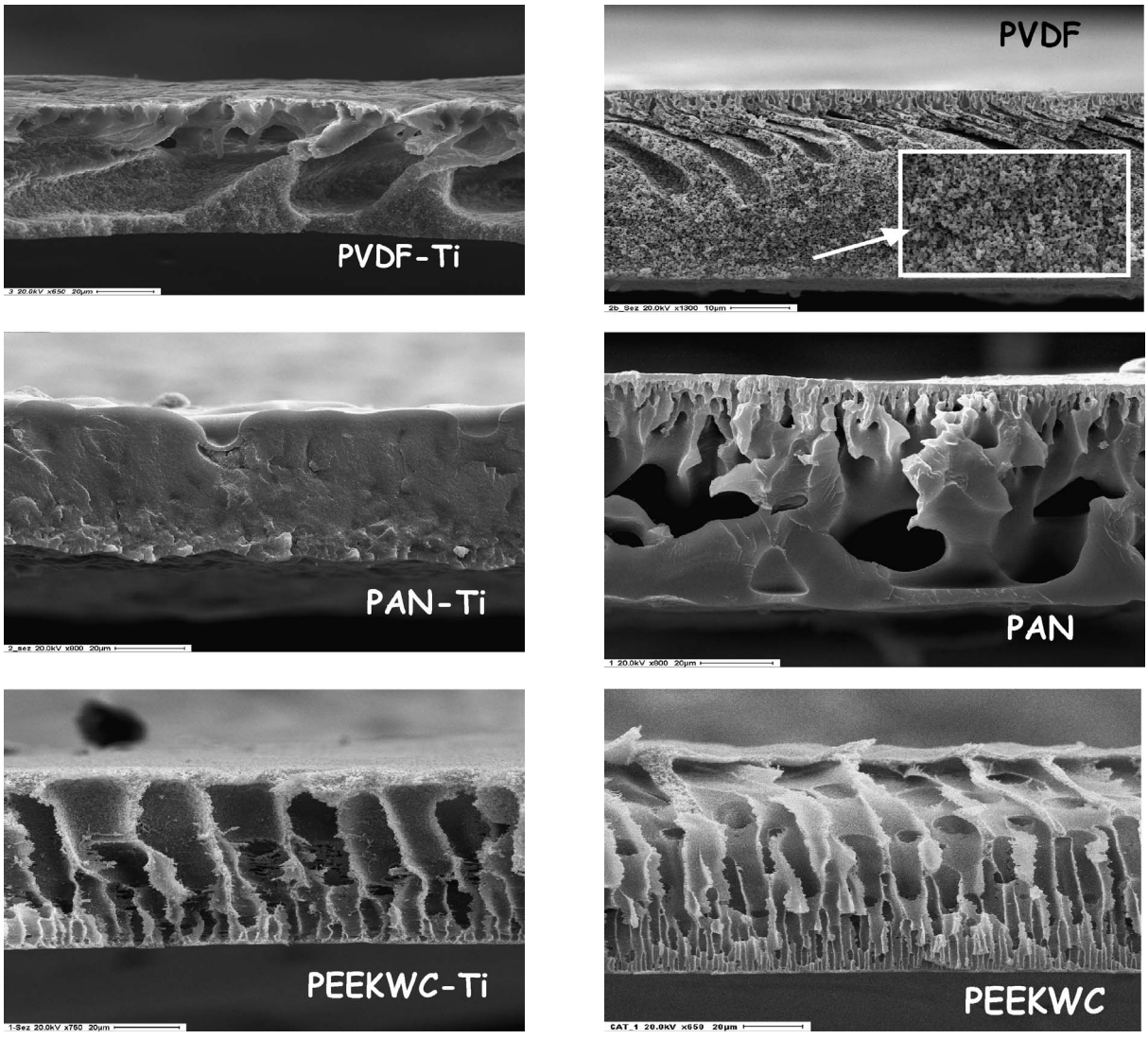

(a) (b)

Fig. 2. SEM photomicrographs of the membranes prepared using PVDF, PAN and PEEKWC (10 wt%) with (a) or without (b) Ti-**2** (1.6 wt%).

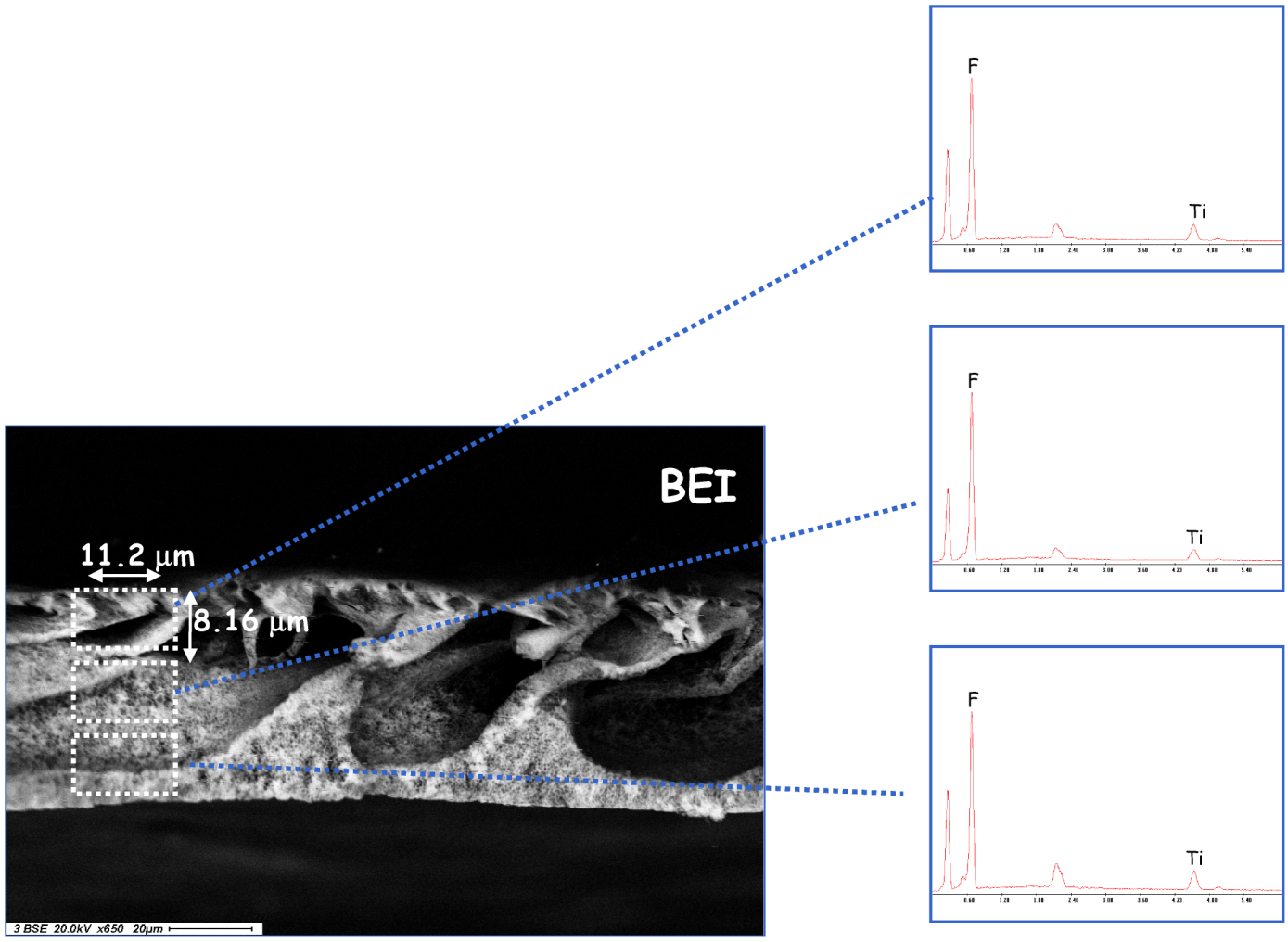

Fig. 3. Cross section of PVDF-Ti membrane in back scattered electron (BSE) mode (a) and corresponding EDX analyses at different depths of membrane cross section (b).

Cross-sections of the polymeric membranes with and without catalyst are shown in Figs. 2a and 2b. According to the synthetic procedure, the catalyst embedding results in the formation of asymmetric hybrid membranes. PEEKWC-Ti membrane has nearly the same morphology of PEEKWC membrane; in both cases, observed asymmetric membranes were characterized by elongated macrovoids. PVDF-Ti membrane has a cavern structure with macrovoids without particulate morphology composed of crystalline particles [32] observed in the analogue PVDF membrane. For membranes synthesized from semicrystalline polymers such as PVDF, crystallization can be enhanced to dominate the precipitation process, thereby yielding particulate morphologies composed of crystalline particles. Of all of the parameters that affect the morphology of precipitated membranes, the composition of the casting solution is the most crucial. In our case, adding the catalyst in the casting solution produced a very unusual morphology without macrovoids, as shown from the morphology in Fig. 2. In addition, for the PAN membranes, different morphologies were observed in the presence of the catalyst in the casting solution. PAN-Ti membrane has a nearly symmetric structure, in contrast to the completely asymmetric PAN membrane. In all likelihood the catalyst delays the liquid–liquid demixing process favoring macrovoid suppression [33].

A uniform catalyst distribution was observed in all of the catalytic polymeric membranes prepared using solvent DMA only in casting solution.

Fig. 3a shows a cross-section of PVDF-Ti membrane in back-scattering mode (BSE). The uniform catalyst distributions were confirmed by EDX analyses of membrane cross-sections. In fact, the intensities of Ti with respect to fluoride peak (chosen as reference) were constant in EDX spectra at different depths of membrane cross-sections (Fig. 3b). Fig. 4 shows the surface of the PVDF-Ti membrane in BSE and the corresponding X-ray maps. The surface was dense and clean. Ti-**2** was observed, suggesting that Ti-**2** was not recrystallized into

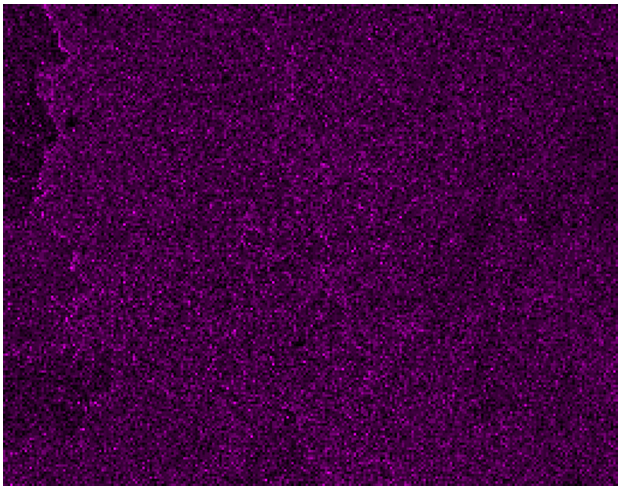

(a)

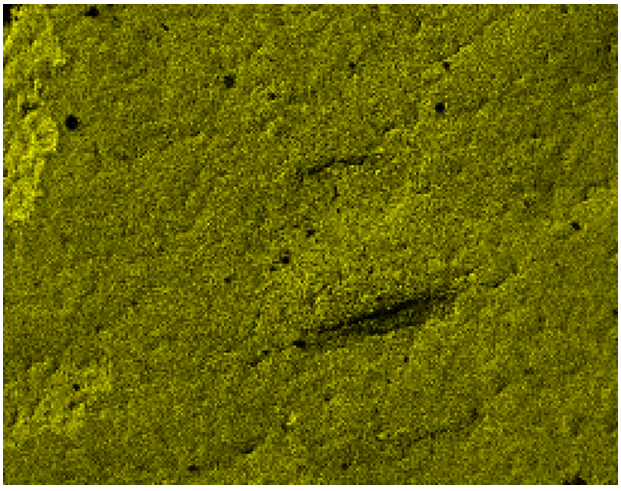

(b)

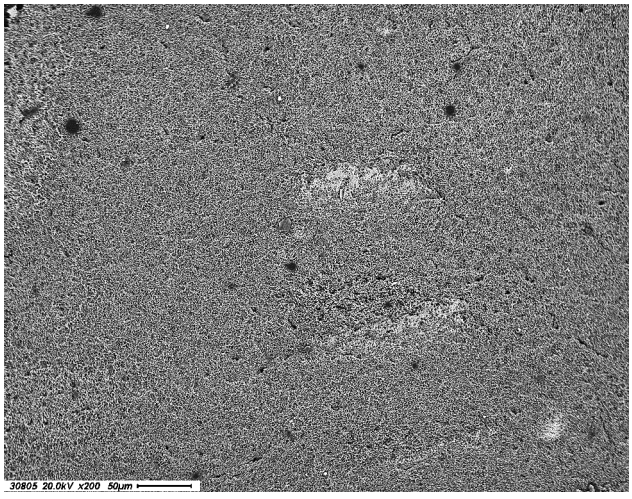

(c)

Fig. 4. X-Ray maps of PVDF-Ti surface (Ti, a; F, b) and corresponding BSE analysis (c).

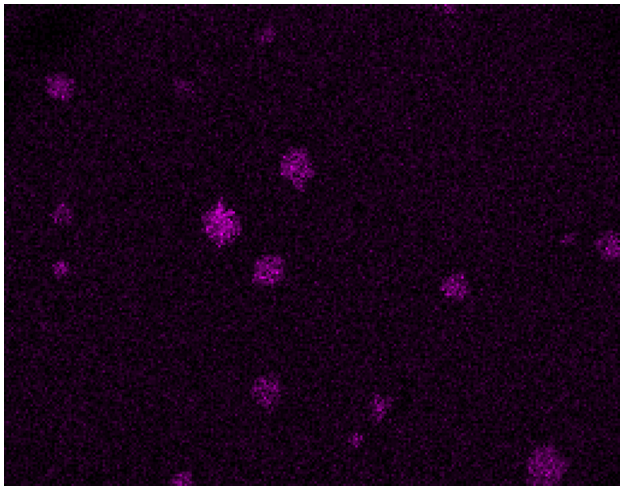

(a)

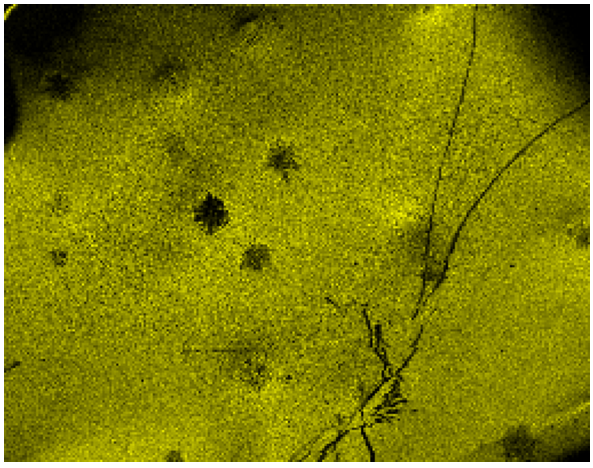

(b)

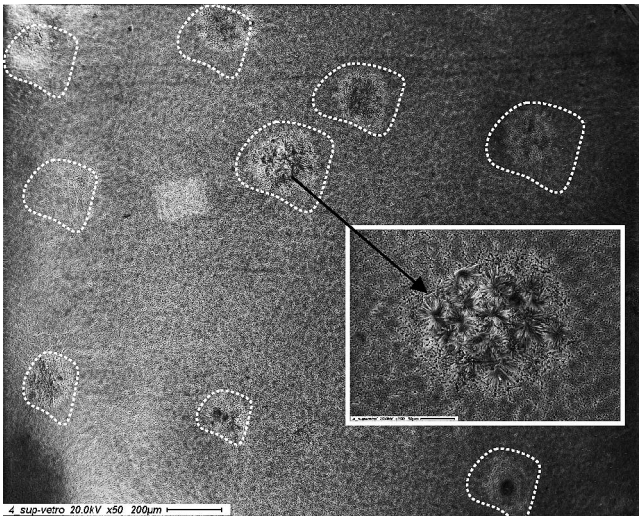

(c)

Fig. 5. Surface characterization of PVDF catalytic membranes prepared by using two solvent in casting solution (DMA and acetone). X-Ray maps of PVDF-Ti surface (Ti, a; F, b) and corresponding BSE analysis (c).

large particles, but rather was highly dispersed as fine particles throughout the polymeric matrix. In contrast, no uniform catalyst distribution was observed in PVDF catalytic membranes prepared using a mixture of two solvents (i.e., DMA and acetone) in the casting solution. However, there are visible large spots (≈150 µm) due to recrystallization of the catalyst on the membrane surface (Fig. 5) These results are explained by the volatility difference between DMA and acetone: Acetone goes out from the nascent membrane for evaporation (dry step), cre-

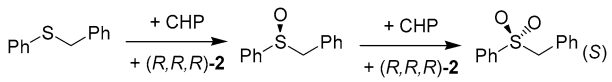

Scheme 3.

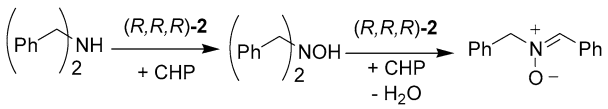

Scheme 4.

Table 2
Oxidation of benzyl phenyl sulfide with CHP catalyzed by Ti(IV) complexes[a]

#	Catalyst	Solvent	Time (h)	Conversion (%)	$SO:SO_2$	e.e. (*S*) (%)
1	Ti(IV)-**2**	DCE	4	94	56:44	69
2	PVDF-Ti	DCE	5	93	59:41	67
3	Ti(IV)-**2**	CH_3CN	1	15	90:10	44
4	PEEKWC-Ti	CH_3CN	100	8	100:0	40

[a] Reaction conditions: $[substrate]_0 = 0.1$ M; $[CHP]_0 = 0.1$ M, [catalyst] = 0.01 M, $T = 0\,^{\circ}C$.

Table 3
Effect of the catalyst on reaction times and product distribution in the Ti-catalyzed oxidation of dibenzylamine with CHP[a]

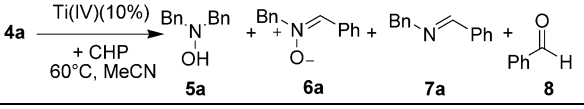

Time (h)	Catalyst (product ratio: **4a**:**5a**:**6a**:**7a**:**8**)			
	Ti-**2**	PVDF-Ti	PAN-Ti	PEEKWC-Ti
3	4:5:74:5:3	38:12:44:6:0	54:6:25:11:4	92:1:6:1:0
7	1:4:78:4:13	0:7:82:5:6	49:6:27:12:7	82:1:14:3:0
25			9:0:40:18:33	58:1:34:7: 0
117				43:2:34:14:6

[a] Reaction conditions: [substrate] = 0.1 M; [CHP] = 0.4 M, [catalyst] = 0.01 M; CD_3CN; $T = 60\,^{\circ}C$.

ating catalyst microdomains on the membrane surface, whereas the membrane final structure is due to DMA/water diffusion in the coagulation bath (wet step).

3.3. Crystal structure of PVDF-based membranes

Both PVDF-based membranes shown in Fig. 2 are inherently crystalline, although their bulk morphologies exhibit different features, as before observed. Identification of the crystalline phases was carried out with FTIR spectroscopy and X-ray diffraction. Fig. 6 shows the FTIR spectra of PVDF-Ti and PVDF membranes. Sharp β-phase characteristic peaks at 470, 511, and 840 cm^{-1} were observed in both membranes. Comparing the IR absorption bands characteristic of the α, β, and γ phases for PVDF reported in the literature [34] shows that PVDF-TI catalytic film and PVDF membranes exhibit the same β-type crystalline phase regardless of the Ti-**2** addition. This was also confirmed by means of XRD spectra (data not shown). The peak at 20.66° is attributed to the reflection of the (110) plane and thus to β-type crystallites [35].

3.4. Membrane activity

Initially, the reactivity of the catalytic membranes was tested in the sulfoxidation reaction to provide indirect information of the nature of the catalyst and active species embedded in the different membranes (Scheme 3). Preliminary tests indicated that catalyst leaching was not a serious problem for the new catalytic membranes. In fact, after the membrane was washed twice with the solvent of the reaction, no significant amount of catalyst or free trialkanolamine ligand could be detected in solution via ^{1}H-NMR.

In the sulfoxidation reaction, due to the occurrence of two cooperative stereoselective processes, (i.e., asymmetric oxidation of the sulfide and subsequent kinetic resolution for the overoxidation to sulfone), the enantiopurity of the sulfoxide increased during the course of the reaction.

The results obtained with PVDF-Ti and PEEKWC-Ti, together with results obtained under homogeneous conditions, are reported in Table 2. It is noteworthy that in both cases the catalytic membranes were able to activate CHP and that (S)-benzyl phenyl sulfoxide was produced with stereoselectivities comparable to those of the homogeneous systems, even if reactivities were rather diverse. Despite the fact that reactions in DCE are intrinsically faster than those in CH_3CN, PVDF-Ti catalytic membrane (Table 2, entry 2) undoubtedly gave the best results, affording high conversion into products with ee's comparable to those of the homogeneous system (Table 2, entry 1). In contrast, PEEKWC-Ti afforded only the sulfoxide in much lower yields (8%) and at much longer reaction times (100 h) (Table 2, entry 3). These data indicate that both membranes maintain catalyst stability and that in the case of more hydrophobic membrane PVDF-Ti, the reactivity of the system is not significantly depleted.

The screening of activity of the different catalytic membranes (PVDF-Ti, PEEKWC-Ti, and PAN-Ti) was also assessed in the oxidation of dibenzylamine, which was chosen as the model substrate (Scheme 4). To better compare the results, the reactions were carried out under the best conditions selected for the homogeneous reactions. Due to the solubility of PEEK-WC in chlorinated solvents (the most suitable solvents for homogeneous reactions), the reactivity was initially explored in acetonitrile, and the course of the reactions was monitored via ^{1}H-NMR. Table 3 reports the product distributions at increasing reaction times for the oxidations catalyzed by PVDF-Ti, PEEKWC-Ti, PAN-Ti, and Ti-**2** homogeneous system. Significantly, all three Ti-based catalytic membranes could activate CHP for the oxygen transfer process, although the polymeric matrix plays an important role in determining performance and product distribution.

Reactions performed with PAN-Ti and PEEK-WC-Ti gave slow conversions of the reagent, giving nitrone in comparable amounts with *N*-benzylidene benzylamine and benzaldehyde. Furthermore, at long reaction times, high amounts of benzaldehyde were recovered due to further oxidation/hydrolysis of the products. In contrast, PVDF-Ti efficiently catalyzed oxidation, giving nitrone in good yields (82%) in reasonable reaction times, almost comparable to those of the homogeneous system.

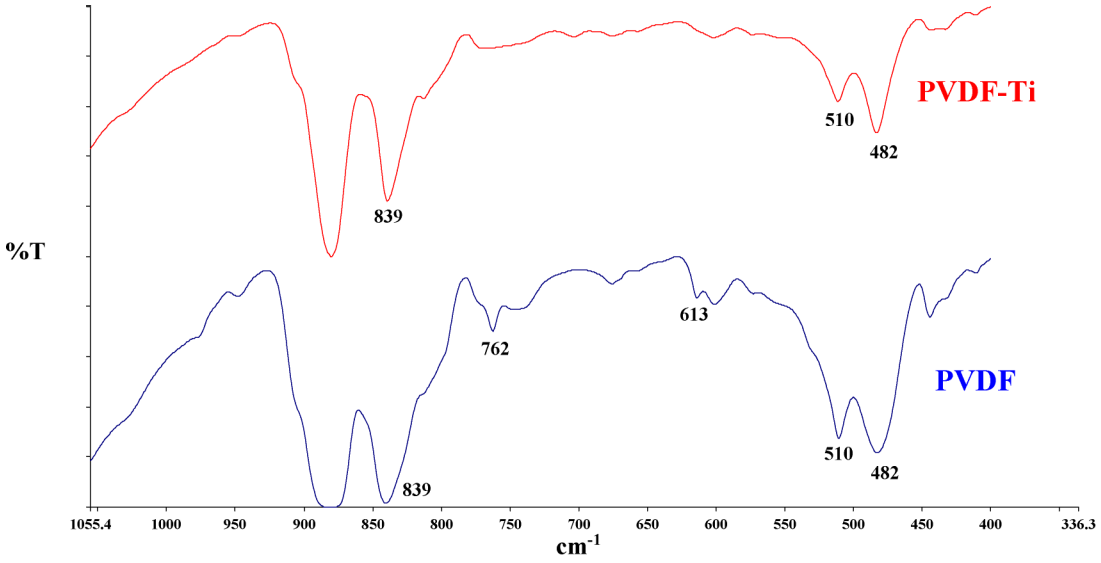

Fig. 6. FTIR spectra of PVDF-Ti and PVDF membranes.

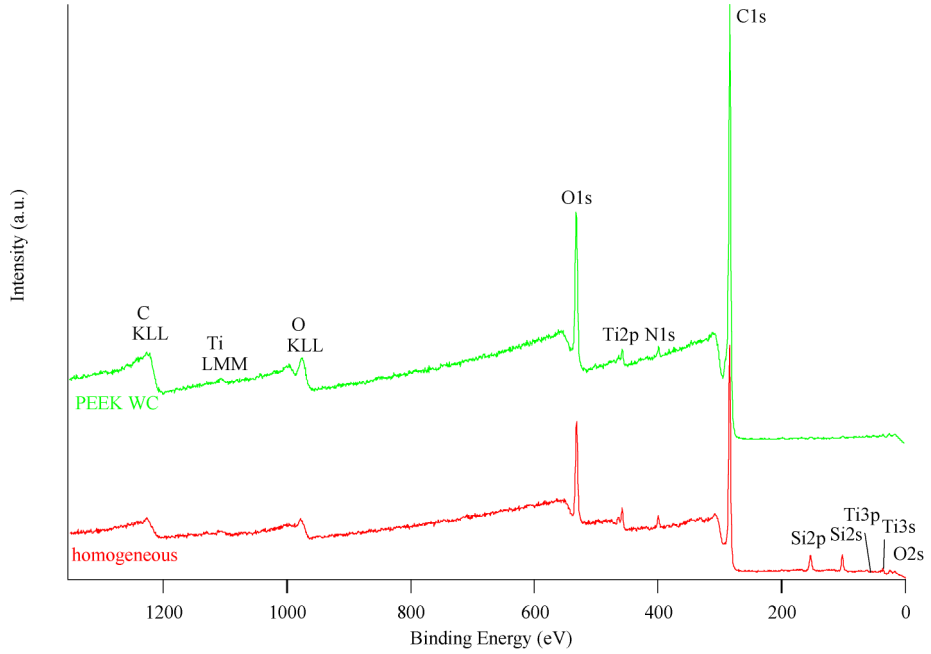

Fig. 7. XPS survey spectra of PEEKWC-Ti membrane and homogeneous catalyst Ti-**2**.

The oxidation with catalytic membrane PVDF-Ti was also tested in chloroform. In chloroform, the reaction occurs much faster ($t_{1/2}(CDCl_3) = 65$ min vs $t_{1/2}(CH_3CN) = 140$ min), and nitrone was recovered at a high chemical yield (92%) with almost complete chemoselectivity (with only traces of imine and hydroxylamine detected).

The performance of the PVDF-Ti catalytic membrane was also evaluated on the basis of system recycling. A series of experiments were performed to examine this membrane's activity along five oxidation runs. After each experiment, the membrane was removed from the reaction vessel, washed in chloroform to remove adsorbed reagent or products, and recycled. The results are reported in Table 4.

Table 4
Oxidation of dibenzylamine with CHP catalyzed by PVDF-Ti, catalyst recycling: substrate: $[substrate]_0 = 0.1$ M; $[CHP]_0 = 0.4$ M, $[catalyst] = 0.01$ M; $T = 60\,^{\circ}C$, $CDCl_3$, m.s. = 250 mg/mmol in run 1, 500 mg/mmol runs 2–5[a]

Run	$T_{1/2}$ (min)	Nitrone (%)
1	39	92
2	10	90
3	14	90
4	14	90
5	23	90

[a] In the recycling, the presence of twice amount of ms proved to be beneficial in decreasing the formation of benzaldehyde.

It is noteworthy that the catalytic activity of the PVDF-Ti membrane was maintained for all five runs, affording compa-

Table 5
Effect of substrate/catalyst ratio on oxidation of dibenzylamine catalyzed by PVDF-Ti membrane or the homogeneous catalyst Ti(IV)-**2** in $CDCl_3$ at 60 °C[a]

$[Sub]_0$, M	Sub/Cat	Catalyst	Time (h)	Nitrone (%)
0.1	10:1	Ti-**2**[b]	3	100
		PVDF-Ti	2.5	92
1.0	100:1	Ti-**2**[b]	1	100
		PVDF-Ti	3	90
1.0	1000:1	Ti-**2**[b]	100	68[c]
		PVDF-Ti	71	65[d]

[a] Conditions: [catalyst] = 0.01 M, dibenzylamine, CHP (4 equiv) and 4A molecular sieves in $CDCl_3$ at 60 °C.
[b] See Ref. [26].
[c] Complete reagent conversion; other products: *N*-benzylidene benzylamine (15%), PhCHO (15%).
[d] Complete reagent conversion; other products: *N*-benzylidene benzylamine (10%), PhCHO (22%). DCE as solvent.

Table 6
Catalytic oxidation of secondary amines by CHP[a]

Substrate	Product	$T_{1/2}$ (min)	Yield[b] (%)
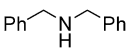	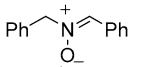	39	92
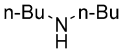	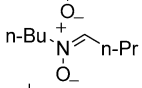	50	80
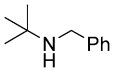	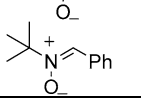	20	93

[a] Reaction conditions: $[substrate]_0 = 0.10$ M, $[CHP]_0 = 0.40$ M; [catalyst] = 0.01 M, 4A molecular sieve, $CHCl_3$ at 60 °C.
[b] Based on isolated product after chromatography. Reactions were carried out on mmol scale. In all cases nitrones were readily isolated in synthetically significant chemical yields (80–93%) via removal of the solvent under vacuum followed by chromatography over silica gel.

rable yields in nitrone (90%). Interestingly, reaction rates were higher in the recycling experiments than in the initial experiment. This increased reactivity could originate from modifications of the polymeric membrane that make available a larger quantity of the catalyst or enhance the Lewis acidity of the metal complex. This important aspect will be addressed in future studies.

The effect of catalyst loading for the PVDF-Ti membrane was also tested at substrate/catalyst ratios of 10:1–1000:1 (Table 5). The results demonstrate that complete conversion of dibenzylamine and >90% selectivity for nitrone could also be achieved in the presence of 1% of catalyst. However, further increasing the ratio to $s/c = 1000$ (which necessarily decreased the catalyst concentration to 0.001 M) resulted in a severe deterioration of chemoselectivity, as was also observed in the homogeneous system [26].

The conditions for the highest catalyst loading (10%) from Table 5 were adopted to explore the scope of the reaction with other secondary amines (Table 6). Benzylic or branched nitrones were highly stable in the oxidative environment; in all cases they were readily isolated in synthetically significant chemical yields (80–93%).

3.5. Contact angle measurements

Our study showed that all of the catalytic membranes preserve the structure of Ti-**2** catalyst, as indirectly observed on the basis of reactivity tests. However, the membrane reactivities are rather diverse. PVDF-Ti gave the best results in terms of conversion and selectivity; in contrast, reactions performed with PAN-Ti and PEEKWC-Ti gave low and slow conversion of the reagent. This difference was ascribed to the different chemical–physical properties of the polymeric membranes (surface tension differences). The catalytic membranes investigated exhibited different values of acidic component γ^+ due to their different chemical structures (Table 7). In fact, as Della Volpe and Siboni suggested, one "cannot compare the acid and base components of the same solvent (or substrate), but eventually the acid (or base) components of different substrates can be compared" [48].

PVDF-Ti exhibited the highest value of γ^+, due to the fluoride atoms of the PVDF. With its acidic character, PVDF probably favors the nucleophilic attack of dibenzylamine more than PEEKWC and PAN do, with lower γ^+ and higher γ^- values, respectively.

3.6. X-Ray photoelectron spectroscopy

The physicochemical interactions of Ti-**2** with the polymeric membrane were explored by XPS analyses. XPS analyses of homogeneous catalyst, PVDF-Ti, and PEEKWC-Ti membranes revealed a unique titanium species present in all of the systems (Figs. 7 and 8). This experimental evidence agrees with the comparable stereoselectivity observed in asymmetric sulfoxidation using these catalytic membranes.

Furthermore, a very peculiar and interesting orientation of the catalyst has been found in the PVDF-Ti membrane. It was possible to obtain quantitative surface analyses by XPS. As shown in Table 8, in the solid catalyst, a Ti/N ratio of about 1.0

Table 7
Contact angles in water (W), glycerol (Gl), diiodomethane (DIM) and calculated surface tension parameters of different catalytic polymeric membranes: γ^{LW} = Lifshitz–van der Waals component, γ^+ = electron-acceptor (acid parameter) component and γ^- = electron (base parameter) of the liquid surface tension γ_S. The surface tension and its parameter were calculated according to Good–Van Oss equation by the average values of measured contact angles

Membrane	ϑDIM (°)	ϑW (°)	ϑGl (°)	γ_S^{LW} (mJ/m^2)	γ_S^- (mJ/m^2)	γ_S^+ (mJ/m^2)	γ_S^{AB} (mJ/m^2)	γ_S (mJ/m^2)
PVDF-Ti	58	123	130	29.5	2.9	9.7	10.6	40.05
PEEKWC-Ti	62	84.2	73	27.4	7.9	0.48	3.8	31.3
PAN-Ti	65	51	54	25.7	32.8	1.75	15.1	40.8

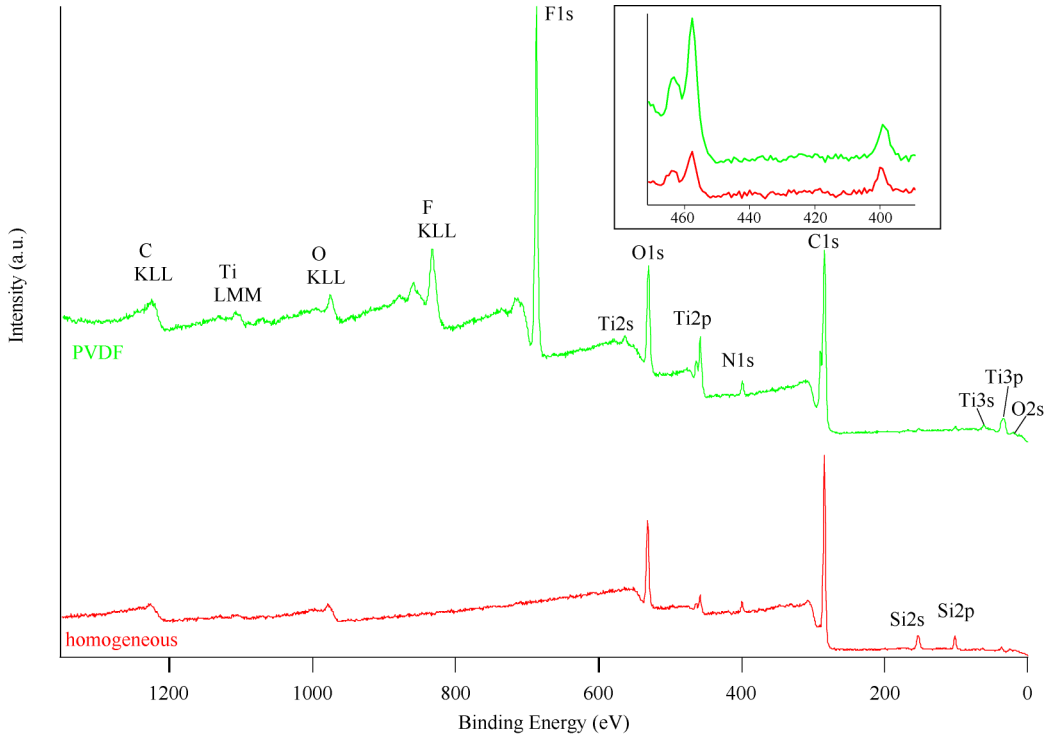

Fig. 8. XPS survey spectra of PVDF-Ti membrane and homogeneous catalyst Ti-**2**.

Table 8
Atomic compositions (%) derived from XPS spectra

Sample	C	O	Si	Cl	F	Ti	N	Ti/N
Ti-**2**	73.7	17.0	5.3	0.2	0.0	1.7	2.1	0.8
PVDF-Ti	57.6	12.1	0.8	0.0	24.7	2.8	2.0	1.5
PEEKWC-Ti	83.1	14.6	0.3	0.0	0.0	0.7	1.3	0.5

Table 9
Atomic compositions (%) of untested and tested PVDF-Ti membranes from angle-dependent XPS spectra

Sample	Composition at 45° take off angle								Composition at 15° take off angle							
	C	O	Si	Cl	F	Ti	N	Ti/N	C	O	Si	Cl	F	Ti	N	Ti/N
PVDF-Ti Untested	57.6	12.1	0.8	0.0	24.7	2.8	2.0	1.5	56.0	12.4	0.0	0.0	26.9	3.1	1.6	1.9
PVDF-Ti After II run	50.9	15.8	1.4	1.5	24.5	3.5	2.4	1.4	51	17.7	1.7	1.4	22.4	4.1	1.8	2.3

(0.8) was found, due to the 1-to-1 titanium–nitrogen stoichiometry. In the PVDF-Ti membrane, a 1.5 Ti/N ratio was found. These results clearly indicate that in this membrane, Ti is more exposed than N on the surface, or, in other words, Ti atoms with the labile monodentate alkoxy ligand lie on the PVDF membrane surface. For the PEEKWC-Ti membrane, a 0.5 ratio was found, indicating that in this case, N is more exposed to the membrane surface than Ti.

We performed a qualitative angle-resolved study to confirm that Ti lies on the surface of PVDF-Ti. As the take-off angle (the angle between the surface and the photoelectrons accepted by the analyzer) decreases, the surface sensitivity of XPS increases [49]. Table 9 gives the atomic compositions derived from survey spectra at two take-off angles of untested and tested (after run II) PVDF-Ti membranes. As expected, the Ti/N ratio increased at lower take-off angles, confirming that the Ti atoms are nearer to the surface than the N atoms. It is noteworthy that after run II, this orientation effect of the Ti-**2** in PVDF-based membrane is enhanced. This result provides important experimental evidence for the observed increased reactivity of PVDF-Ti after run II.

4. Conclusion

In this work we have achieved the first heterogenization of Ti(IV) catalysts. Polymeric catalytic membranes consisting of Ti(IV)/trialkanolamine complex entrapped in PVDF, PAN, and PEEKWC membranes are active for the oxidation of dibenzylamine to nitrone. For all of the catalytic membranes, SEM, EDX, and BSE analyses exhibited a uniform catalyst distri-

bution. XRD and FTIR analyses showed that the crystalline structure of PVDF-Ti was unchanged by addition of the catalyst.

The reactivity screening allowed us to: (i) select the PVDF-Ti catalytic membrane as the best system in terms of conversion and selectivity, (ii) exclude the occurrence of competing homogeneous pathways, and (iii) recycle the catalytic membrane for five runs without loss of activity. XPS analyses done to explore the nature of the catalyst embedded in the polymeric matrices confirmed the preservation of the catalyst structure based on reactivity tests. A very interesting orientation of the Ti(IV) complex was observed on the PVDF membrane surface, which is the origin of the higher activity of PVDF-Ti compared with that of the analogue homogeneous system.

In addition, analyses of the surface acid parameters (γ^+) of the PVDF-, PEEKWC-, and PAN-based catalytic membranes provides a supporting argument for the observed differences in reactivity. PVDF-Ti membranes exhibited the highest value of γ^+, due to the fluoride atoms of the PVDF. This may favor nucleophilic attack of the substrate compared with the PEEKWC-Ti and PAN-Ti membranes, with lower γ^+ values and higher γ^- values, respectively.

Acknowledgments

The authors are grateful to the Italian Ministry of University and Research for supporting this research through the MIUR-FIRB RBNE03JCR5 project.

References

[1] A.T. Bell, Science 299 (2003) 1688.
[2] M.A. Barteau, J.E. Lyons, I.K. Song, J. Catal. 216 (2003) 236.
[3] J. Corker, Science 271 (1996) 966.
[4] V. Vidal, A. Theolier, J. Thivolle-Cazat, J.M. Basset, Science 276 (1997) 99.
[5] C. Nozkaki, C.G. Lugmair, A. Bell, T.D. Tilley, J. Am. Chem. Soc. 124 (2002) 13194.
[6] D. Kolb, Surf. Sci. 500 (2002) 722.
[7] K.P. De Jong, J.W. Geus, Catal. Rev. Sci. Eng. 42 (2000) 481.
[8] D. Fritch, K.-V. Peinemann, Catal. Today 25 (1995) 277.
[9] J.F. Ciebien, R.E. Cohen, A. Duran, Supramol. Sci. 5 (1998) 31.
[10] J. Vital, A.M. Ramos, I.F. Silva, H. Valente, J. E Castanheiro, Catal. Today 56 (2000) 167.
[11] I.F.J. Vankelecom, N.M.F. Moens, K.A.L. Vercruysse, R.F. Parton, P.A. Jacobs, in: H.U. Blaser, A. Baiker, R. Prins (Eds.), Heterogeneous Catalysis and Fine Chemicals, IV, Elsevier, Amsterdam, 1997, p. 437.
[12] I.F.J. Vankelecom, Chem. Rev. 102 (2002) 3779.
[13] P.E.F. Neys, A. Severeyns, I.F.J. Vankelecom, E. Ceulemans, W. Dehaen, P.A. Jacobs, J. Mol. Catal. 144 (1999) 373.
[14] I.F.J. Vankelecom, P.A. Jacobs, Catal. Today 56 (2000) 147.
[15] P.E.F. Neys, I.F.J. Vankelecom, R.F. Parton, W. Dehaen, G. L'abbé, P.A. Jacobs, J. Mol. Catal. 126 (1997) L9.
[16] R.F. Parton, I.F.J. Vankelecom, D. Tas, K.B. Janssen, P.P. Knops-Gerrits, P.A. Jacobs, J. Mol. Catal. 113 (1996) 283.
[17] I.F.J. Vankelecom, D. Tas, R.F. Parton, V. Van de Vyver, P.A. Jacobs, Angew. Chem. Int. Engl. 35 (1996) 1346.
[18] P.P. Knops-Gerrits, I.F.J. Vankelecom, E. Beatse, P.A. Jacobs, Catal. Today 32 (1996) 63.
[19] M.C. Carreno, Chem. Rev. 95 (1995) 1717.
[20] P. Pichen, Asymmetric Synthesis of Sulfoxides: Two Case Studies in Chirality in Industry II, Wiley, New York, 1997, p. 381.
[21] F.P. Ballistreri, U. Chiacchio, A. Rescina, G. Tomaselli, R.M. Toscano, Tetrahedron 48 (1992) 8677.
[22] F.P. Ballistreri, R. Bianchini, C. Pinzino, G. Tomaselli, R.M. Toscano, J. Phys. Chem. A 104 (2000) 2710.
[23] W.A. Nugent, R.L. Harlow, J. Am. Chem. Soc. 116 (1994) 6142.
[24] F. Di Furia, G. Licini, G. Modena, R. Motterle, W.A. Nugent, J. Org. Chem. 61 (1996) 5175.
[25] G. Licini, M. Bonchio, G. Modena, W.A. Nugent, Pure Appl. Chem. 71 (1999) 463.
[26] M. Forcato, W.A. Nugent, G. Licini, Tetrahedron Lett. 44 (2003) 49.
[27] K. Jian, P.N. Pintauro, J. Membr. Sci. 85 (1993) 301.
[28] R.J. Good, C.J. van Oss, in: M.E. Scrader, G.L. Loeb (Eds.), Modern Approaches to Wettability, Plenum, New York, 1992.
[29] C.J. van Oss, Interfacial Forces in Aqueous Media, Dekker, New York, 1994.
[30] A. Bottino, G. Camera Roda, G. Capannelli, S. Munari, J. Membr. Sci. 57 (1991) 1.
[31] H.K. Lonsdale, J. Membr. Sci. 10 (1982) 81.
[32] J.H. Kim, B.R. Min, J. Won, H.C. Park, Y. Kang, J. Membr. Sci. 187 (2001) 47.
[33] F.M. Gray, Solid Polymer Electrolytes, VCH, New York, 1991.
[34] W.M. Prest, D.J. Luca, J. Appl. Phys. 46 (1975) 4136.
[35] R. Hasegawa, Y. Takahashi, Y. Chatani, H. Tadokoro, Polymer 3 (1972) 600.
[36] R.D. Lundberg, F.E. Bailey, R.W. Callard, J. Polym. Sci. A 1 (4) (1966) 1563.
[37] H.C. Shih, Y.S. Yeh, H. Yasuda, J. Membr. Sci. 50 (1990) 299.
[38] A. Bottino, G. Capannelli, O. Monticelli, P. Piaggio, J. Membr. Sci. 166 (2000) 231.
[39] D. Lin, C. Chang, F.M. Huang, L.P. Cheng, Polymer 44 (2003) 413.
[40] B. Jung, J.K. Yoon, B. Kim, H.W. Rhee, J. Membr. Sci. 243 (2004) 45.
[41] Y. Xiuli, C. Hangbin, W. Xiu, Y. Yongxin, J. Membr. Sci. 146 (1998) 179.
[42] N. Scharnagal, H. Buschtz, Desalination 139 (2001) 191.
[43] S. Yang, Z. Liu, J. Membr. Sci. 222 (2003) 87.
[44] E. Drioli, H.C. Zhang, Chimicaoggi 11 (1989) 59.
[45] F. Tasselli, J.C. Jansen, E. Drioli, J. Appl. Polym. Sci. 91 (2004) 841.
[46] M.G. Buonomenna, A. Figoli, J.C. Jansen, E. Drioli, J. Appl. Polym. Sci. 92 (2004) 576.
[47] M. Mulder, Basic Principles of Membrane Technology, Kluwer, Dordrecht, 1991.
[48] C. Della Volpe, S. Siboni, J. Colloid Interface Sci. 195 (1997) 121.
[49] D. Briggs, M.P. Seah, Practical Surface Analysis, Wiley, Chichester, 1983.